Publication Year	2019
Acceptance in OA@INAF	2021-02-26T17:22:56Z
Title	Addressing the circularity problem in the Ep-Eiso correlation of gamma-ray bursts
Authors	AMATI, LORENZO; D'Agostino, Rocco; Luongo, Orlando; Muccino, Marco; TANTALO, MARIA
DOI	10.1093/mnrasl/slz056
Handle	http://hdl.handle.net/20.500.12386/30660
Journal	MONTHLY NOTICES OF THE ROYAL ASTRONOMICAL SOCIETY. LETTERS
Number	486

Addressing the circularity problem in the $E_\mathrm{p} - E_\mathrm{iso}$ correlation of Gamma-Ray Bursts

Lorenzo Amati,[1]$\star$ Rocco D'Agostino,[2]† Orlando Luongo,[3,4]‡
Marco Muccino,[3]§ Maria Tantalo[5]¶

[1]*INAF, Istituto di Astrofisica Spaziale e Fisica Cosmica, Bologna, Via Gobetti 101, I-40129 Bologna, Italy.*
[2]*Sezione INFN, Università di Roma "Tor Vergata", Via della Ricerca Scientifica 1, I-00133, Roma, Italy.*
[3]*Istituto Nazionale di Fisica Nucleare, Laboratori Nazionali di Frascati, 00044 Frascati, Italy.*
[4]*NNLOT, Al-Farabi Kazakh National University, Al-Farabi av. 71, 050040 Almaty, Kazakhstan.*
[5]*Dipartimento di Fisica, Università di Roma "Tor Vergata", Via della Ricerca Scientifica 1, I-00133, Roma, Italy.*

ABSTRACT

We here propose a new model-independent technique to overcome the circularity problem affecting the use of Gamma-Ray Bursts (GRBs) as distance indicators through the use of E_p–E_iso correlation. We calibrate the E_p–E_iso correlation and find the GRB distance moduli that can be used to constrain dark energy models. We use observational Hubble data to approximate the cosmic evolution through Bézier parametric curve obtained through the linear combination of Bernstein basis polynomials. In so doing, we build up a new data set consisting of 193 GRB distance moduli. We combine this sample with the supernova JLA data set to test the standard ΛCDM model and its wCDM extension. We place observational constraints on the cosmological parameters through Markov Chain Monte Carlo numerical technique. Moreover, we compare the theoretical scenarios by performing the AIC and DIC statistics. For the ΛCDM model we find $\Omega_m = 0.397^{+0.040}_{-0.039}$ at the 2σ level, while for the wCDM model we obtain $\Omega_m = 0.34^{+0.13}_{-0.15}$ and $w = -0.86^{+0.36}_{-0.38}$ at the 2σ level. Our analysis suggests that ΛCDM model is statistically favoured over the wCDM scenario. No evidence for extension of the ΛCDM model is found.

Key words: gamma-ray bursts: general – cosmology: dark energy – cosmology: observations

1 INTRODUCTION

The cosmic speed up is today a consolidate experimental evidence confirmed by several probes (Haridasu, Luković, D'Agostino & Vittorio 2017). Particularly, type Ia Supernovae (SNe Ia) have been employed as standard candles (Phillips 1993) to check the onset of cosmic acceleration (Perlmutter et al., 1998, 1999; Riess et al., 1998; Schmidt et al., 1998). Their importance lies in the fact that they may open a window into the nature of the constituents pushing up the universe to accelerate. Even though SNe Ia are considered among the most reliable standard candles, they are detectable at most at redshifts $z \simeq 2$ (Rodney et al., 2015). Thus, at intermediate

redshifts the standard cosmological model, dubbed the ΛCDM paradigm, cannot be tested with SNe Ia alone. Consequently, higher redshift distance indicators, such as Baryon Acoustic Oscillations (BAO) (Percival et al., 2010; Aubourg et al., 2015; Luković, D'Agostino & Vittorio 2016), have been used to alleviate degeneracy among the ΛCDM paradigm and dark energy scenarios. In these respects, a relevant example if offered by Gamma-Ray Bursts (GRBs), which represent the most powerful cosmic explosions detectable up to $z = 9.4$ (Salvaterra et al., 2009; Tanvir et al., 2009; Cucchiara et al., 2011). Attempts to use GRBs as cosmic rulers led cosmologists to get several correlations between GRB photometric and spectroscopic properties (Amati et al., 2002; Ghirlanda, Ghisellini, Lazzati & Firmani 2004; Amati, Guidorzi, Frontera, Della Valle, Finelli, Landi & Montanari 2008; Schaefer 2007; Capozziello & Izzo 2008; Dainotti, Cardone & Capozziello 2008; Bernardini, Margutti, Zaninoni & Chincarini 2012; Amati & Della Valle 2013; Wei, Wu, Melia, Wei & Feng

$\star$ lorenzo.amati@inaf.it
† rocco.dagostino@roma2.infn.it
‡ orlando.luongo@lnf.infn.it
§ marco.muccino@lnf.infn.it
¶ maria.tantalo@lnf.infn.it

2014; Izzo, Muccino, Zaninoni, Amati & Della Valle 2015; Demianski, Piedipalumbo, Sawant & Amati 2017a,b). The most investigated correlations involve the rest-frame spectral peak energy E_p, i.e. the rest-frame photon energy at which the νF_ν spectrum of the GRB peaks, and the bolometric isotropic-equivalent radiated energy E_{iso}, or peak luminosity L_p (Amati et al. 2002; Yonetoku, Murakami, Nakamura, Yamazaki, Inoue & Ioka 2004; Amati et al. 2008; Amati & Della Valle 2013; Demianski et al. 2017a,b). However, the use of GRBs for cosmology is still affected by some uncertainties due to selection and instrumental effects and the so-called *circularity problem* (see, e.g., Kodama, Yonetoku, Murakami, Tanabe, Tsutsui & Nakamura 2008). The former issue has been investigated in several studies, with the general, even though still debated, conclusion that these effects should be minor (see, e.g., Amati 2006; Ghirlanda, Ghisellini & Firmani 2006; Nava et al., 2012; Amati & Della Valle 2013; Demianski et al. 2017a). The circularity problem arises from the fact that, given the lack of very low-redshift GRBs, the correlations between radiated energy or luminosity and the spectral properties are established assuming a background cosmology. For example, calibrating GRBs through the standard ΛCDM model, the estimate of cosmological parameters of any dark energy framework inevitably returns an overall agreement with the concordance model.

In this paper, we propose a new model-independent calibration of the E_p–E_{iso} correlation (the *Amati relation* see e.g., Amati et al. 2008; Amati & Della Valle 2013). We take the most recent values of observational Hubble Data (OHD), consisting of 31 points of Hubble rates got at different redshifts (see Capozziello, D'Agostino & Luongo 2018, and references therein). These data have been obtained through the differential age method applied to pairs of nearby galaxies, providing model-independent measurements (Jimenez & Loeb 2002). We follow the strategy to fit OHD data using a Bézier parametric curve obtained through the linear combination of Bernstein basis polynomials. This treatment is a refined approximated method and reproduces Hubble's rate at arbitrary redshifts without assuming an *a priori* cosmological model. We thus use it to calibrate the E_{iso} values by means of a data set made of 193 GRBs (with firmly measured redshift and spectral parameters taken from Demianski et al. 2017a and references therein), and compute the corresponding GRB distance moduli μ_{GRB} and the 1σ error bars, depending upon the uncertainties on GRB observables. Detailed discussions of possible biases and selection effects can be found, e.g. in Amati & Della Valle (2013), Demianski et al. (2017a) and Dainotti & Amati (2018). From the above model-independent analysis over OHD data, we obtain $H_0 = 67.74$ km s^{-1} Mpc^{-1}, compatible with the current estimates by the Planck Collaboration et al., (2018) and Riess et al., (2018).

As a pure example of fitting procedure, we analyze our data by means of Markov Chain Monte Carlo (MCMC) technique and compare them with the standard cosmological paradigm and its simplest extension, namely the wCDM model. We discuss the limits over our technique in view of the most recent bias and problems related to SN Ia and GRBs. Afterwards, using the above value of
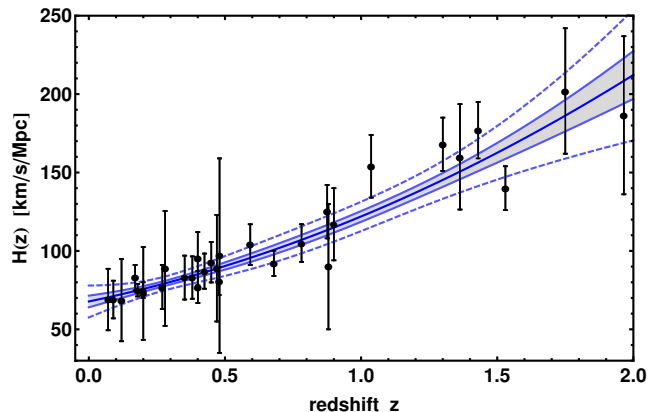

Figure 1. OHD data (31 black points with vertical error bars), their best fit function (solid thick blue curve) and its 1σ (blue curves and light blue shaded are) and 3σ (blue dashed curves) confidence regions.

H_0 got from our parametric fit analysis, we show that our results are in tension with the concordance paradigm (Planck Collaboration et al. 2018) at $\geq 3\sigma$. However, we propose that such results may be affected by systematics and how these limits may be reconsidered in view of future developments. Finally, we compare the statistical performance of the cosmological models through the Bayesian selection criteria.

The paper is divided into four sections. After this Introduction, in Sec. 2 we describe the main features of our treatment, using OHD data surveys over the Amati relation. In Sec. 3, we discuss our numerical outcomes concerning the use of our new data set. We thus get constraints over the free parameters of the ΛCDM and wCDM models. In Sec. 4, we draw conclusions and identify the perspectives of our work.

2 MODEL-INDEPENDENT CALIBRATION OF THE AMATI RELATION

Calibrating the Amati relation represents a challenge due to the problem of circularity (see, e.g., Ghirlanda et al. 2004; Ghirlanda et al. 2006; Kodama et al. 2008; Amati & Della Valle 2013). In fact, in the E_p–E_{iso} correlation, the cosmological parameters Ω_i and the Hubble constant H_0 enter in the E_{iso} definition through the luminosity distance d_L, i.e., $E_{iso}(z, H_0, \Omega_i) \equiv 4\pi d_L^2(z, H_0, \Omega_i) S_{bolo}/(1+z)$, where S_{bolo} is the observed bolometric GRB fluence and the factor $(1+z)^{-1}$ transforms the observed GRB duration into the source cosmological rest-frame one. The most quoted approach to the calibration of the Amati relation makes use of the SN Ia Hubble diagram, directly inferred from the observations, and interpolate it to higher redshift by using GRBs (see, e.g., Kodama et al. 2008; Liang, Xiao, Liu & Zhang 2008; Demianski et al. 2017a,b). However, this method biases the GRB Hubble diagram by introducing the systematics of the SNe Ia.

Here, we propose an alternative calibration which makes use of the *differential age method* based on spectroscopic measurements of the age difference Δt and redshift difference Δz of couples of passively evolving galaxies that formed at the same time (Jimenez & Loeb 2002). This method
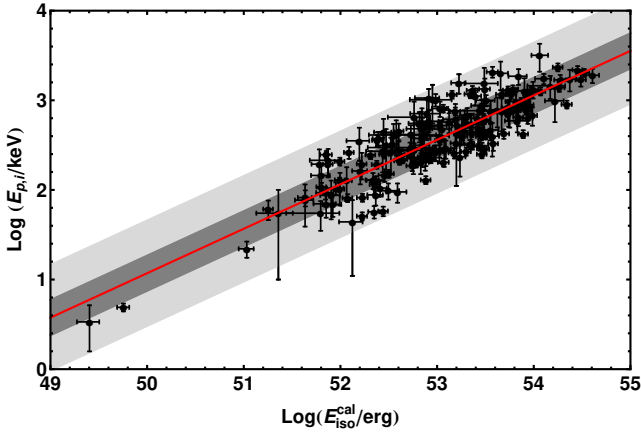
Figure 2. GRB calibrated distribution in the E_p–$E_{\rm iso}^{\rm cal}$ plane (black datapoints), the best-fitting function (red solid line) and the $1\sigma_{\rm ex}$ and $3\sigma_{\rm ex}$ limits (dark-gray and light-gray shaded regions, respectively).

Table 1. Priors used for parameters estimate in the MCMC analysis.

w	Ω_m	M	Δ_M	α	β
$(-0.5, -1.5)$	$(0, 1)$	$(-20, -18)$	$(-1, 1)$	$(0, 1)$	$(0, 5)$

implies that $\Delta z / \Delta t \equiv dz/dt$ and hence the Hubble function can be computed in a cosmology-independent way as $H(z) = -(1 + z)^{-1} \Delta z / \Delta t$. The updated sample of 31 OHD (see Capozziello et al. 2018) is shown in Fig. 1. To avoid the circularity problem, we approximate the OHD data by employing a Bézier parametric curve[1] of degree n

$$H_n(z) = \sum_{d=0}^{n} \beta_d h_n^d(z) \quad , \quad h_n^d(z) \equiv \frac{n!(z/z_{\rm m})^d}{d!(n-d)!} \left(1 - \frac{z}{z_{\rm m}}\right)^{n-d},$$
(1)

where β_d are coefficients of the linear combination of Bernstein basis polynomials $h_n^d(z)$, positive in the range $0 \leq z/z_{\rm m} \leq 1$, where $z_{\rm max}$ is the maximum z of the OHD dataset. For $d = 0$ and $z = 0$, we easily identify $\beta_0 \equiv H_0$. Besides the simple cases with $n = 0$ and $n = 1$ leading to a constant value and a linear growth with z of $H(z)$, respectively, the only case providing a monotonic growing function over the limited range in redshift of the OHD data is $n = 2$; higher values lead to oscillatory behaviors of the approximating function. Therefore, in the following we use $n = 2$ in fitting the OHD data. The best fit with its 1σ and 3σ confidence regions are shown in Fig. 1. The best-fit parameters are $H_0 = 67.76 \pm 3.68$, $\beta_1 = 103.34 \pm 11.14$, and $\beta_2 = 208.45 \pm 14.29$ (all in units of km s^{-1} Mpc^{-1}). The value of H_0 so obtained is compatible with the current estimate of the Planck Collaboration (Planck Collaboration et al. 2018) and in agreement at the 1.49σ level with the value measured by Riess et al. (2018).

Once the function $H_2(z)$ is extrapolated to redshift $z > z_{\rm m}$, the luminosity distance is (see, e.g., Goobar & Perlmutter 1995)

$$d_{\rm L}(\Omega_k, z) = \frac{c}{H_0} \frac{(1 + z)}{\sqrt{|\Omega_k|}} S_k \left[\sqrt{|\Omega_k|} \int_0^z \frac{H_0 dz'}{H_2(z')}\right],$$
(2)

where Ω_k is the curvature parameter, and $S_k(x) = \sinh(x)$ for $\Omega_k > 0$, $S_k(x) = x$ for $\Omega_k = 0$, and $S_k(x) = \sin(x)$ for $\Omega_k < 0$. We note that $d_{\rm L}$ in Eq. (2) is not completely

independent from cosmological scenarios, since it depends upon Ω_k. However, supported by the most recent Planck results (Planck Collaboration et al. 2018), which find $\Omega_k = 0.001 \pm 0.002$, we can safely assume $\Omega_k = 0$. In so doing, the dependency upon Ω_k identically vanishes and Eq. (2) becomes cosmology-independent:

$$d_{\rm cal}(z) = c(1 + z) \int_0^z \frac{dz'}{H_2(z')}.$$
(3)

We are now in the position to use $d_{\rm cal}(z)$ to calibrate the isotropic energy $E_{\rm iso}^{\rm cal}$ for each GRB fulfilling the Amati relation[2]

$$E_{\rm iso}^{\rm cal}(z) \equiv 4\pi d_{\rm cal}^2(z) S_{\rm bolo}(1 + z)^{-1},$$
(4)

where the respective errors $\sigma E_{\rm iso}^{\rm cal}$ depend upon the GRB systematics on the observables and the fitting procedure (see confidence regions in Fig. 1). The corresponding E_p–$E_{\rm iso}^{\rm cal}$ distribution is displayed in Fig. 2. Following the method by D'Agostini (2005), we fit the calibrated Amati relation by using a linear fit $\log(E_p/1{\rm keV}) = q + m[\log(E_{\rm iso}^{\rm cal}/{\rm erg}) - 52]$. We find the best-fit parameters $q = 2.06 \pm 0.03$, $m = 0.50 \pm 0.02$, and the extra-scatter $\sigma_{\rm ex} = 0.20 \pm 0.01$ dex (see Fig. 2). The corresponding Spearman's rank correlation coefficient is $\rho_s = 0.84$ and the p-value from the two-sided Student's t-distribution is $p = 2.42 \times 10^{-36}$.

We can then compute the GRB distance moduli from the standard definition $\mu_{\rm GRB} = 25 + 5 \log(d_{\rm cal}/{\rm Mpc})$. Using the fit of the calibrated Amati relation, we obtain

$$\mu_{\rm GRB} = 25 + \frac{5}{2} \left[\frac{\log E_p - q}{m} - \log\left(\frac{4\pi S_{\rm bolo}}{1 + z}\right) + 52\right],$$
(5)

where now $S_{\rm bolo}$ has been normalized to erg Mpc^{-2} to obtain $d_{\rm cal}$ in the desiderd units of Mpc. The attached errors on $\mu_{\rm GRB}$ take into account the GRB systematics and the statistical errors on q, m and $\sigma_{\rm ex}$. The distribution of $\mu_{\rm GRB}$ with z is shown in Fig. 3

We note that the statistical method adopted for the GRBs calibration may be in principle used also for the analysis of the SN data. This would in fact reduce the propagation errors when the combined fit of both data sets is performed, making the joint sample homogeneous for the cosmological studies. It will be interesting to analyze the impact of such a procedure in a forthcoming study, where the Philips relation of SN will be calibrated in the way we attempted with GRBs prior to performing the cosmological fit.

---

[1] Bézier curves are easy to use in computation, are stable at the lower degrees of control points and can be rotated and translated by performing the operations on the points.

[2] Recent works claim that our universe has non-zero curvature and that Ω_k represents at most the 2% of the total universe energy density (see, e.g., Ooba, Ratra & Sugiyama 2018, and references therein). Relaxing the assumption $\Omega_k = 0$, since its value is still very small, the circularity problem is not completely healed, but it is only restricted to the value of Ω_k, since $H(z)$ can be still approximated by the function $H_2(z)$.
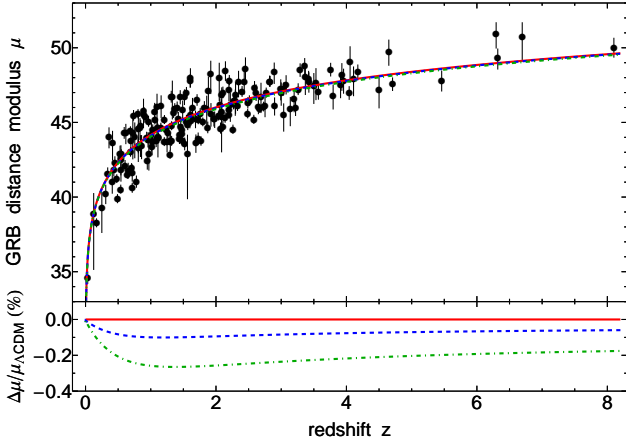
Figure 3. *Upper plot*: GRB distance moduli μ_{GRB} distribution compared to the ΛCDM model $\mu_{\Lambda\mathrm{CDM}}$ with $H_0 = 67.36$ km s^{-1} Mpc^{-1}, $\Omega_m = 0.3166$ and $\Omega_\Lambda = 0.6847$ as in Planck Collaboration et al. (2018) (solid red curve), and two wCDM models with the above ΛCDM parameters and $w = -0.90$ (dashed blue curve) and $w = -0.75$ (dot-dashed green curve). *Lower plot*: the deviations of the above three models μ_X from $\mu_{\Lambda\mathrm{CDM}}$ computed as $(\mu_X - \mu_{\Lambda\mathrm{CDM}})/\mu_{\Lambda\mathrm{CDM}}$ (curves retain the same meaning as before).

3 NUMERICAL RESULTS

We here use our sample of GRBs to test cosmological models. In particular, we assume standard barotropic equation of state (EoS). Thus, for each fluid the pressure P_i is a one-to-one function of the density ρ_i: $P_i = w_i \rho_i$. As a consequence of Bianchi's identity, one gets $\dot\rho_i + 3H\rho_i(1 + w_i) = 0$ for each species entering the Einstein equations. Following the standard recipe, we here consider pressureless matter with negligible radiation and define current total density as $\Omega_i = \rho_i/\rho_c$, with $\rho_c \equiv 8\pi G/(3H_0^2)$ is the critical density, one can reformulate the Hubble evolution as:

$$H(z) = H_0\sqrt{\Omega_m(1+z)^3 + \Omega_{DE}(1+z)^{3(1+w)}} \ . \qquad (6)$$

In the above relation, dark energy takes a net density given by $\Omega_{DE} = 1 - \Omega_m$ to guarantee that $H(z = 0) = H_0$, and w is the dark energy EoS parameter. In particular, Eq. (6) reduces to the ΛCDM model as $w = -1$, whereas to the wCDM model when w is free to vary. The distance modulus is given by $\mu_{th}(z) = 25 + 5\log[d_L(z)/\mathrm{Mpc}]$, where $d_L(z)$ is given by Eq. (2) with $\Omega_k = 0$. Thus, the likelihood function of the GRB data can be written as

$$\mathcal{L}_{\mathrm{GRB}} = \prod_{i=1}^{N_{\mathrm{GRB}}} \frac{1}{\sqrt{2\pi}\sigma_{\mu_{\mathrm{GRB},i}}} \exp\left[-\frac{1}{2}\left(\frac{\mu_{th}(z_i) - \mu_{\mathrm{GRB},i}}{\sigma_{\mu_{\mathrm{GRB},i}}}\right)^2\right], \qquad (7)$$

where $N_{\mathrm{GRB}} = 193$ is the number of GRB data points. To obtain more robust observational bounds on cosmological parameters, we consider a complete Hubble diagram by complementing the GRB measurements with the SN JLA sample (Betoule et al. 2014). The latter consists of 740 SN Ia in the redshift range $0.01 < z < 1.3$. The distance modulus of each SN is parameterized as

$$\mu_{\mathrm{SN}} = m_B - M_B + \alpha X_1 - \beta C \ , \qquad (8)$$

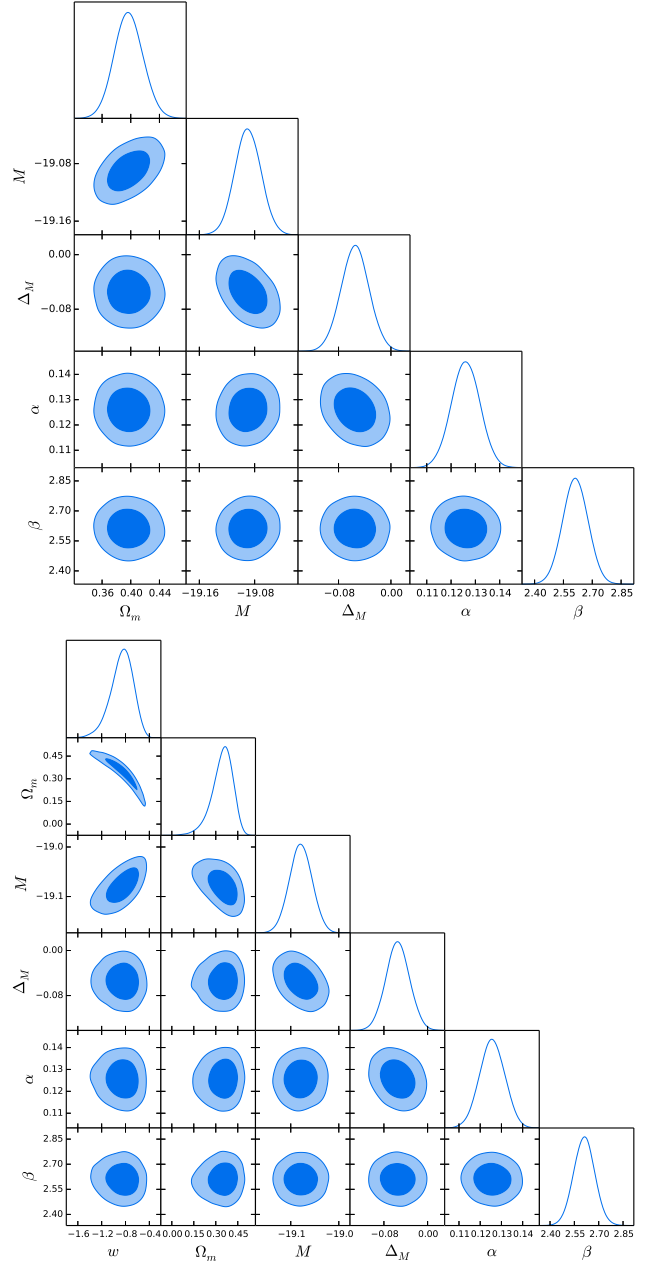where m_B is the B-band apparent magnitude, while C and X_1 are the colour and the stretch factor of the light curve,

Figure 4. Marginalized 1σ and 2σ contours, and posterior distributions from the MCMC analysis of SN+GRB data for the ΛCDM model (top) and for the wCDM model (bottom).

respectively; M_B is the absolute magnitude defined as

$$M_B = \begin{cases} M & \text{if } M_{host} < 10^{10} M_{Sun} \ , \\ M + \Delta_M & \text{otherwise} \ , \end{cases} \qquad (9)$$

where M_{host} is the host stellar mass, and M, α and β are nuisance parameters which enter the fits along with cosmological parameters. The likelihood function of the SN data is given as

$$\mathcal{L}_{SN} = \frac{1}{|2\pi\mathcal{M}|^{1/2}} \exp\left[-\frac{1}{2}(\mu_{th} - \mu_{\mathrm{SN}})^{\mathrm{T}} \mathcal{M}^{-1} (\mu_{th} - \mu_{\mathrm{SN}})\right], \qquad (10)$$

Table 2. 95% confidence level results of the MCMC analysis for the SN+GRB data. The AIC and DIC differences are intended with respect to the ΛCDM model.

Model	w	Ω_m	M	Δ_M	α	β	ΔAIC	ΔDIC
ΛCDM	-1	$0.397^{+0.040}_{-0.039}$	$-19.090^{+0.037}_{-0.037}$	$-0.055^{+0.043}_{-0.043}$	$0.126^{+0.011}_{-0.012}$	$2.61^{+0.13}_{-0.13}$	0	0
wCDM	$-0.86^{+0.36}_{-0.38}$	$0.34^{+0.13}_{-0.15}$	$-19.079^{+0.046}_{-0.046}$	$-0.055^{+0.042}_{-0.042}$	$0.126^{+0.011}_{-0.012}$	$2.61^{+0.13}_{-0.13}$	1.44	1.24

where $\mathcal{M}$ is the $3N_{\rm SN} \times N_{\rm SN} = 2220 \times 2200$ covariance matrix with the statistical and systematic uncertainties on the light-curve parameters given in Betoule et al. (2014).

We thus perform a MCMC integration on the combined likelihood function $\mathcal{L} = \mathcal{L}_{\rm SN}\mathcal{L}_{\rm GRB}$ by means of the Metropolis-Hastings algorithm implemented through the Monte Python code (Audren, Lesgourgues, Benabed & Prunet 2013). In the numerical procedure, we assume uniform priors on the fitting parameters (see Table 1) and we take H_0 as the best-fit value obtained from the model-independent analysis of the OHD data: $H_0 = 67.74$ km/s/Mpc. We summarize the results for the ΛCDM and wCDM models in Table 2. We show the marginalized 1σ and 2σ confidence contours in Fig. 4. One immediately sees that Ω_m in the ΛCDM model is unusually high compared to previous findings which use SNe Ia and other surveys different from GRBs. In fact, our result is in tension with Planck's predictions (Planck Collaboration et al. 2018) at $\geq 3\sigma$. However, our outcome is well consistent within 1σ with previous analyses which made use of GRBs (see. e.g. Amati & Della Valle 2013 for a review, and Izzo et al. 2015, Haridasu et al. 2017 and Demianski et al. 2017a,b for recent results). In addition, the tension is reduced as one considers the wCDM model, enabling w to vary. This does not indicate that wCDM is favoured with respect to the standard cosmological model. In fact, we immediately notice that w is consistent within 1σ with the ΛCDM case, i.e. $w = -1$.

We note that the numerical approach using the Metropolis-Hasting algorithm may suffer from some issues related to random walk behaviour. In the case of highly correlated statistical models, the use of more robust integration methods could alleviate many of those issues. Alternative approaches for the multi-level structure of the proper Bayesian model are left for a future study.

3.1 Statistical performances with GRBs

To test the statistical performance of the models under study, we apply the AIC criterion (Akaike 1974):

$$\text{AIC} \equiv 2p - 2\ln\mathcal{L}_{max},$$

where p is the number of free parameters in the model and $\mathcal{L}_{max}$ is the maximum probability function calculated at the best-fit point. The best model is the one that minimizes the AIC value. We also use the DIC criterion (Kunz, Trotta & Parkinson 2006) defined as

$$\text{DIC} \equiv 2p_{eff} - 2\ln\mathcal{L}_{max},$$

where $p_{eff} = \langle -2\ln\mathcal{L}\rangle + 2\ln\mathcal{L}_{max}$ is the number of parameters that a dataset can effectively constrain. Here, the brackets indicate the average over the posterior distribution. Un-like the AIC and BIC criteria, the DIC statistics does not penalize for the total number of free parameters of the model, but only for those which are constrained by the data (Liddle 2007). We thus computed the differences with respect to the reference ΛCDM flat scenario. Both the AIC and DIC results indicate that the ΛCDM model is only slightly favoured with respect to the wCDM model (see Table 2).

4 FINAL OUTLOOKS AND PERSPECTIVES

In this work, we faced out the circularity problem in using GRBs as distance indicators. To do so, we employed the $E_{\rm p} - E_{\rm iso}$ ("Amati") correlation and we proposed a new technique to build d_L in a model-independent way, using the OHD measurements. In particular, we considered the OHD data points and we approximated the Hubble function by means of a Bézier parametric curve obtained from the linear combinations of Bernstein's polynomials. Assuming vanishing spatial curvature as suggested by Planck's results, we were able to calibrate the Amati relation in a model-independent way. We thus obtained a new sample of distance moduli for 193 different GRBs (see Table 1).

We then used the new data sample to constrain two different cosmological scenarios: the concordance ΛCDM model, and the wCDM model, with the dark energy EoS parameter is free to vary. Hence, we performed a Monte Carlo integration through the Metropolis-Hastings algorithm on the joint likelihood function obtained by combining the GRB measurements with the SNe JLA data set. In our numerical analysis, we fixed H_0 to the best-fit value obtained from the model-independent analysis over OHD data, i.e. $H_0 = 67.74$ km s^{-1} Mpc^{-1}. Our results for Ω_m and w agree with previous findings making use of GRBs and our treatment candidates as a severe alternative to calibrate the Amati relation in a model-independent form. Finally, we employed the AIC and BIC selection criteria to compare the statistical performance of the investigated models. We found that the ΛCDM model is preferred with respect to the minimal wCDM extension. Although a pure ΛCDM model is statistically favoured, we note that the values of Ω_m and w for the wCDM model are remarkably in agreement with those obtained by the Dark Energy Survey (DES) (Abbott et al. 2018). We can then conclude that no modifications of the standard paradigm are expected as intermediate redshifts are involved.

Future efforts will be dedicated to the use of our new technique to fix refined constraints over dynamical dark energy models. Also, we will compare our outcomes with respect to previous model-independent calibrations.

ACKNOWLEDGEMENTS

REFERENCES

Abbott T. M. C., et al., 2018
Amati L., 2006, MNRAS, 372, 233
Amati L., Della Valle M., 2013, International Journal of Modern Physics D, 22, 1330028
Amati L., et al., 2002, A&A, 390, 81
Amati L., Guidorzi C., Frontera F., Della Valle M., Finelli F., Landi R., Montanari E., 2008, MNRAS, 391, 577
Aubourg É., et al., 2015, Phys. Rev. D, 92, 123516
Audren B., Lesgourgues J., Benabed K., Prunet S., 2013, J. Cosmology Astropart. Phys., 2, 001
Bernardini M. G., Margutti R., Zaninoni E., Chincarini G., 2012, MNRAS, 425, 1199
Betoule M., et al., 2014, A&A, 568, A22
Capozziello S., Izzo L., 2008, A&A, 490, 31
Capozziello S., D'Agostino R., Luongo O., 2018, MNRAS, 476, 3924
Cucchiara A., et al., 2011, ApJ, 736, 7
D'Agostini G., 2005, ArXiv Physics e-prints,
Dainotti M. G., Amati L., 2018, Publications of the Astronomical Society of the Pacific, 130, 051001
Dainotti M. G., Cardone V. F., Capozziello S., 2008, MNRAS, 391, L79
Demianski M., Piedipalumbo E., Sawant D., Amati L., 2017a, A&A, 598, A112
Demianski M., Piedipalumbo E., Sawant D., Amati L., 2017b, A&A, 598, A113
Ghirlanda G., Ghisellini G., Lazzati D., Firmani C., 2004, ApJ, 613, L13
Ghirlanda G., Ghisellini G., Firmani C., 2006, New Journal of Physics, 8, 123
Goobar A., Perlmutter S., 1995, ApJ, 450, 14
Haridasu B. S., Luković V. V., D'Agostino R., Vittorio N., 2017, Astron. Astrophys., 600, L1
Izzo L., Muccino M., Zaninoni E., Amati L., Della Valle M., 2015, A&A, 582, A115
Jimenez R., Loeb A., 2002, ApJ, 573, 37
Kodama Y., Yonetoku D., Murakami T., Tanabe S., Tsutsui R., Nakamura T., 2008, MNRAS, 391, L1
Kunz M., Trotta R., Parkinson D., 2006, Phys. Rev., D74, 023503
Liang N., Xiao W. K., Liu Y., Zhang S. N., 2008, ApJ, 685, 354
Liddle A. R., 2007, Mon. Not. Roy. Astron. Soc., 377, L74
Luković V. V., D'Agostino R., Vittorio N., 2016, A&A, 595, A109
Nava L., et al., 2012, MNRAS, 421, 1256
Ooba J., Ratra B., Sugiyama N., 2018, ApJ, 864, 80
Percival W. J., et al., 2010, MNRAS, 401, 2148
Perlmutter S., et al., 1998, Nature, 391, 51
Perlmutter S., et al., 1999, ApJ, 517, 565
Phillips M. M., 1993, ApJ, 413, L105
Planck Collaboration et al., 2018, arXiv e-prints, p. arXiv:1807.06209
Riess A. G., et al., 1998, AJ, 116, 1009
Riess A. G., et al., 2018, ApJ, 861, 126
Rodney S. A., et al., 2015, AJ, 150, 156
Salvaterra R., et al., 2009, Nature, 461, 1258
Schaefer B. E., 2007, ApJ, 660, 16
Schmidt B. P., et al., 1998, ApJ, 507, 46
Tanvir N. R., et al., 2009, Nature, 461, 1254
Wei J.-J., Wu X.-F., Melia F., Wei D.-M., Feng L.-L., 2014, MNRAS, 439, 3329
Yonetoku D., Murakami T., Nakamura T., Yamazaki R., Inoue A. K., Ioka K., 2004, ApJ, 609, 935

This paper has been typeset from a TeX/LaTeX file prepared by the author.

Table 1. List of the full sample of GRBs used in this work and their redshift z and calibrated $\mu_{\rm GRB}$.

GRB	z	$\mu_{\rm GRB} \pm \sigma_{\mu,{\rm GRB}}$	GRB	z	$\mu_{\rm GRB} \pm \sigma_{\mu,{\rm GRB}}$	GRB	z	$\mu_{\rm GRB} \pm \sigma_{\mu,{\rm GRB}}$	GRB	z	$\mu_{\rm GRB} \pm \sigma_{\mu,{\rm GRB}}$
970228	0.695	43.76 ± 0.77	051109A	2.346	47.73 ± 0.89	090323	3.57	47.08 ± 0.53	120909A	3.93	48.20 ± 0.93
970508	0.835	44.64 ± 0.73	060115	3.5328	47.67 ± 1.07	090328	0.736	45.47 ± 0.36	121128A	2.2	45.56 ± 0.30
970828	0.958	43.87 ± 0.51	060124	2.296	46.47 ± 0.88	090418A	1.608	48.05 ± 0.64	130408A	3.758	48.55 ± 0.46
971214	3.42	47.97 ± 0.51	060206	4.0559	49.11 ± 1.22	090423	8.1	50.05 ± 0.67	130420A	1.297	42.87 ± 0.29
980613	1.096	46.06 ± 1.11	060210	3.91	47.52 ± 0.79	090424	0.544	42.67 ± 0.30	130427A	0.3399	41.59 ± 0.41
980703	0.966	45.09 ± 0.37	060218	0.03351	34.60 ± 0.42	090516	4.109	47.93 ± 1.00	130505A	2.27	46.27 ± 0.39
981226	1.11	44.03 ± 1.13	060306	3.5	47.48 ± 1.04	090618	0.54	40.54 ± 0.30	130518A	2.488	46.31 ± 0.37
990123	1.6	45.37 ± 0.70	060418	1.489	45.89 ± 0.64	090715B	3.	47.01 ± 0.78	130701A	1.155	44.69 ± 0.30
990506	1.3	43.74 ± 0.57	060526	3.22	45.97 ± 0.50	090812	2.452	48.61 ± 0.88	130831A	0.4791	41.24 ± 0.30
990510	1.619	45.14 ± 0.34	060607A	3.075	47.57 ± 0.65	090902B	1.822	46.04 ± 0.40	131011A	1.874	44.68 ± 0.39
990705	0.842	43.51 ± 0.73	060614	0.125	38.88 ± 2.58	090926	2.1062	44.75 ± 0.35	131030A	1.295	43.82 ± 0.31
990712	0.434	41.85 ± 0.44	060707	3.424	47.74 ± 0.68	090926B	1.24	44.51 ± 0.30	131105A	1.686	45.26 ± 0.59
991208	0.706	41.98 ± 0.31	060729	0.543	42.55 ± 1.22	091003	0.8969	45.53 ± 0.52	131108A	2.4	47.08 ± 0.36
991216	1.02	43.36 ± 0.52	060814	1.9229	45.63 ± 0.79	091018	0.971	42.94 ± 1.05	131117A	4.042	46.99 ± 0.46
000131	4.5	47.18 ± 1.04	060908	1.8836	47.14 ± 1.18	091020	1.71	46.52 ± 0.39	131231A	0.642	41.55 ± 0.30
000210	0.846	44.82 ± 0.34	060927	5.46	47.84 ± 0.70	091024	1.092	43.92 ± 0.32	140206A	2.73	46.07 ± 0.33
000418	1.12	43.97 ± 0.35	061007	1.262	44.36 ± 0.41	091029	2.752	46.12 ± 0.68	140213A	1.2076	43.72 ± 0.30
000911	1.06	45.76 ± 0.58	061121	1.314	46.73 ± 0.40	091127	0.49	39.90 ± 0.31	140419A	3.956	47.83 ± 0.84
000926	2.07	44.62 ± 0.37	061126	1.1588	46.15 ± 0.76	091208B	1.063	45.18 ± 0.30	140423A	3.26	47.24 ± 0.40
010222	1.48	44.52 ± 0.34	061222A	2.088	46.87 ± 0.51	100414A	1.368	45.92 ± 0.37	140506A	0.889	45.78 ± 0.99
010921	0.45	42.29 ± 0.49	070125	1.547	45.08 ± 0.44	100621A	0.542	41.88 ± 0.41	140508A	1.027	43.69 ± 0.32
011121	0.36	44.03 ± 0.70	070521	1.35	45.67 ± 0.36	100728A	1.567	44.83 ± 0.34	140512A	0.725	44.31 ± 1.41
011211	2.14	45.34 ± 0.35	071003	1.604	47.79 ± 0.45	100728B	2.106	47.03 ± 0.39	140515A	6.32	49.32 ± 0.71
020124	3.198	46.59 ± 0.79	071010B	0.947	42.48 ± 0.59	100814A	1.44	43.93 ± 0.36	140518A	4.707	47.58 ± 0.46
020405	0.69	43.02 ± 0.31	071020	2.145	48.45 ± 0.66	100816A	0.8049	45.58 ± 0.31	140620A	2.04	45.44 ± 0.30
020813	1.25	43.73 ± 0.67	071117	1.331	46.77 ± 1.30	100906A	1.727	43.93 ± 0.41	140623A	1.92	48.26 ± 1.12
020819B	0.41	41.07 ± 0.75	080207	2.0858	45.41 ± 1.78	101213A	0.414	43.63 ± 1.00	140629A	2.275	46.46 ± 0.50
020903	0.25	39.31 ± 1.38	080319B	0.937	44.01 ± 0.36	101219B	0.55	42.89 ± 0.31	140801A	1.32	44.79 ± 0.30
021004	2.3	46.86 ± 1.06	080411	1.03	44.50 ± 0.38	110206A	0.618	44.31 ± 0.68	140808A	3.29	48.53 ± 0.45
021211	1.01	44.21 ± 0.97	080413A	2.433	47.75 ± 0.78	110205A	2.22	46.20 ± 0.98	140907A	1.21	45.20 ± 0.30
030226	1.98	45.23 ± 0.55	080413B	1.1	44.63 ± 0.70	110213A	1.46	44.71 ± 0.79	141028A	2.33	46.12 ± 0.35
030323	3.37	48.08 ± 1.06	080603B	2.69	46.77 ± 1.02	110213B	1.083	43.79 ± 0.43	141109A	2.993	47.27 ± 0.71
030328	1.52	43.58 ± 0.43	080605	1.64	46.00 ± 0.65	110422A	1.77	43.76 ± 0.32	141220A	1.3195	43.78 ± 0.33
030329	0.1685	38.28 ± 0.30	080607	3.036	47.24 ± 0.44	110503A	1.613	45.56 ± 0.34	141221A	1.452	46.71 ± 0.47
030429	2.65	46.09 ± 0.50	080721	2.591	47.33 ± 0.46	110715A	0.82	43.42 ± 0.30	141225A	0.915	45.43 ± 0.41
030528	0.78	41.06 ± 0.41	080804	2.2045	47.83 ± 0.35	110731A	2.83	47.76 ± 0.37	150206A	2.087	45.71 ± 0.44
040912B	1.563	42.91 ± 2.16	080913	6.695	50.73 ± 1.26	110801A	1.858	45.94 ± 1.06	150301B	1.5169	46.73 ± 0.52
040924	0.859	43.48 ± 0.81	080916A	0.689	44.44 ± 0.30	110818A	3.36	48.79 ± 0.56	150314A	1.758	45.62 ± 0.35
041006	0.716	41.64 ± 0.57	080928	1.6919	43.64 ± 0.62	111107A	2.893	48.38 ± 0.72	150323A	0.593	44.32 ± 0.40
041219	0.31	40.24 ± 0.65	081007	0.5295	42.92 ± 0.59	111228A	0.716	40.63 ± 0.34	150403A	2.06	46.20 ± 0.42
050318	1.4436	44.22 ± 0.52	081008	1.9685	45.26 ± 0.49	120119A	1.728	45.22 ± 0.34	150413A	3.139	45.92 ± 0.98
050401	2.8983	46.12 ± 0.61	081028	3.038	45.51 ± 0.95	120326A	1.798	45.04 ± 0.30	150514A	0.807	43.47 ± 0.43
050416A	0.6535	41.8 ± 0.54	081118	2.58	45.21 ± 0.30	120624B	2.1974	45.89 ± 0.47	150821A	0.755	44.07 ± 1.20
050525A	0.606	42.13 ± 0.36	081121	2.512	46.48 ± 0.34	120711A	1.405	46.00 ± 0.40	151021A	1.49	43.82 ± 0.36
050603	2.821	47.76 ± 0.37	081203A	2.05	47.99 ± 1.28	120712A	4.1745	48.38 ± 0.53	151027A	0.81	44.57 ± 1.31
050820	2.615	47.03 ± 0.55	081221	2.26	44.55 ± 0.31	120716A	2.486	45.60 ± 0.32	151029A	1.423	45.24 ± 0.51
050904	6.295	50.94 ± 0.88	081222	2.77	47.00 ± 0.34	120724A	1.48	44.25 ± 0.68			
050922C	2.199	47.20 ± 0.73	090102	1.547	47.01 ± 0.37	120802A	3.796	46.82 ± 0.84			
051022	0.809	43.30 ± 0.82	090205	4.6497	49.78 ± 0.88	120811C	2.671	45.95 ± 0.30			